

HYLON_TNF_2025_05_Phase2-1: Dataset Hydrogen/Air flames in a dual swirl coaxial injector: Geometry and operating conditions at atmospheric pressure

S. Marragou, M. Vilespy, Z. Al Hadi, A. Teixeira, H. Magnes, L. Selle,
G. Magnotti, T. Guiberti, T. Poinso, T. Schuller

11 May 2025

Version of the database: **HYLON_TNF_2025_05_Phase2-1**

When downloading the database, please contact us at poinso@cerfacs.fr to be added to the mail list and be informed of updates.

Table 1: [Table of releases.](#)

Date	Release name	Description
20 April 2025	HYLON_TNF_2025_Phase2-1	Initial version
11 May 2025	HYLON_TNF_2025_05_Phase2-1	Initial version + Wall temperature data

1 Update HYLON_TNF_2025_05_Phase2-1

Previous version of the TNF dataset: HYLON_TNF_2025_Phase2-1

The update HYLON_TNF_2025_05_Phase2-1 includes additional data. The changes are listed below:

- The nomenclature of the flames has been modified for clarity when high pressure data will be released.
- The temperature measurements of the both quartz and steel walls, and of the backplane have been added, with a description of the experimental setup and the data.

2 Abstract

This file provides documentation on the measurements conducted at Institut de Mécanique des Fluides de Toulouse (IMFT) and King Abdullah University of Science and Technology (KAUST) with the HYLON burner [11, 10, 9, 5, 1, 7, 3, 4, 8, 6, 12], a dual swirl co-axial injector for H_2 /air combustion.

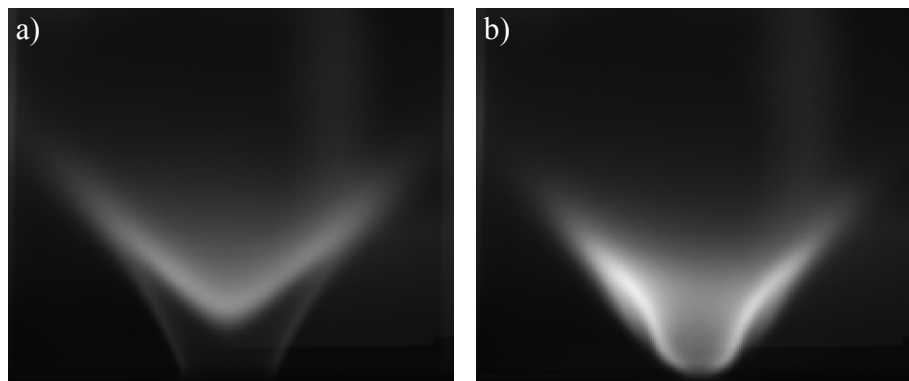


Figure 1: Flame pictures of: (a) Flame A.1 (attached) and (b) Flame L.1 (lifted).

Air and H_2 are injected separately into coaxial tubes equipped with axial swirlers. Two operating points were studied, corresponding to the flames shown in Figure 1. The flame A.1 (Figure 1.a) is anchored to the injector lips, and the flame L.1 is lifted above the injector lips (Figure 1.b). This document describes the burner geometry and the operating conditions for the two flames chosen for the database of the phase 2.1 of the TNF HYLON database. The name of the folder corresponds to the version of the data file, referenced as `HYLON_TNF_YEAR_Phase2-1-UpdtX` for the Update number X made available at year YEAR. Example: `HYLON_TNF_2025_Phase2-1-Updt1` for the update1 made available in 2025.

Phase 2.1 is carried out with a slightly modified version of the HYLON burner used in the previous TNF database, adapted for operation at elevated pressure: if you computed Phase 1, corresponding to **HYLON_TNF_2023_****, you need to reconstruct a new mesh.

Flames A.1 and L.1 correspond to the two first flame databases which will be available for atmospheric pressure conditions. Higher pressure data will come next in 2025 and will be added in the next versions of the document. The experimental setup and operating conditions are described in the Section 3. The numerical domain is described in Section 4. Publications associated to this database are synthesized in Section 7.

3 Experimental setup description

3.1 HYLON v2 geometry

For HYLON_TNF_2025_Phase2-1, experiments were conducted with a new version of the HYLON (HYdrogen LOw NOx) injector [11, 10, 9, 5, 1, 7, 3, 4, 8, 6, 12] with a radial to axial swirling vane in the air channel and a beveled lip in an inverted conical shape for the hydrogen injector as the one used in Magnes *et al.* [3, 4] and Marragou *et al.* [6] as illustrated in Figure 2. It is a H₂/air dual swirl coaxial injector where hydrogen is injected through the central tube and air through the annular tube. The air swirler yields a swirl number of $S_e = 1.2$ estimated from geometrical considerations. The inner swirl number is estimated to be $S_i = 0.6$ with the same considerations.

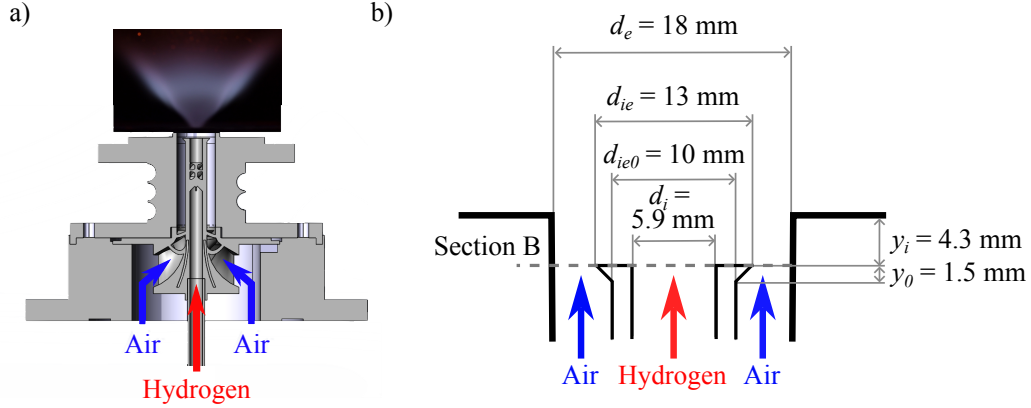


Figure 2: Schematic (a) of the HYLON injector of HYLON_TNF_2025_Phase2-1 and main dimensions (b).

Both swirl motions are in a clockwise direction from a top point of view of the injector. The main dimensions of the injector are given in Figure 2.b. The inner diameter of the central hydrogen channel is $d_i = 6$ mm and the outer diameter of the annular air channel is $d_e = 18$ mm. The central tube has an initial external diameter of $d_{ie0} = 10$ mm and enlarges linearly in the radial direction to $d_{ie} = 13$ mm in the last $z_0 = 1.5$ mm upstream of the outlet of the central hydrogen tube. The outlet of the central hydrogen tube is recessed by $z_i = 4.3$ mm upstream of the outlet of the annular air channel. The main dimensions of the injector are reported in Table 2. Downstream of the injector, a square combustion chamber with a close to 360° optical access was installed. The chamber has a length of 145 mm and a width of 78 mm. A converging nozzle from a square to a round section was placed at the top of the combustion chamber with a contraction ratio of 0.51 to avoid the dilution of burnt gases inside the combustion chamber with air entrained from outside the combustor. Bulk velocity values are calculated at Section B, as defined by the dimensions indicated in Figure 2.b, for an injection temperature fixed to $T_{IN} = 298$ K and a pressure equal to the atmospheric value $p = 1$ bar.

Table 2: Main dimensions of the injector.

d_i [mm]	d_{ie0} [mm]	d_{ie} [mm]	d_e [mm]	z_i [mm]	z_0 [mm]	α_{si} [°]	α_{se} [°]
5.9	10	13	18	4.3	1.5	51	61

3.2 Global flow properties: swirl number

It is interesting to evaluate the level of swirl using a simplified method based on the swirler geometry. The methodology, the assumptions and the resulting equation for the swirl number calculation are detailed below. Only the final expression is given here. Notations refer to Figure 3 and values of the main dimensions of the injector are reported in Table 2

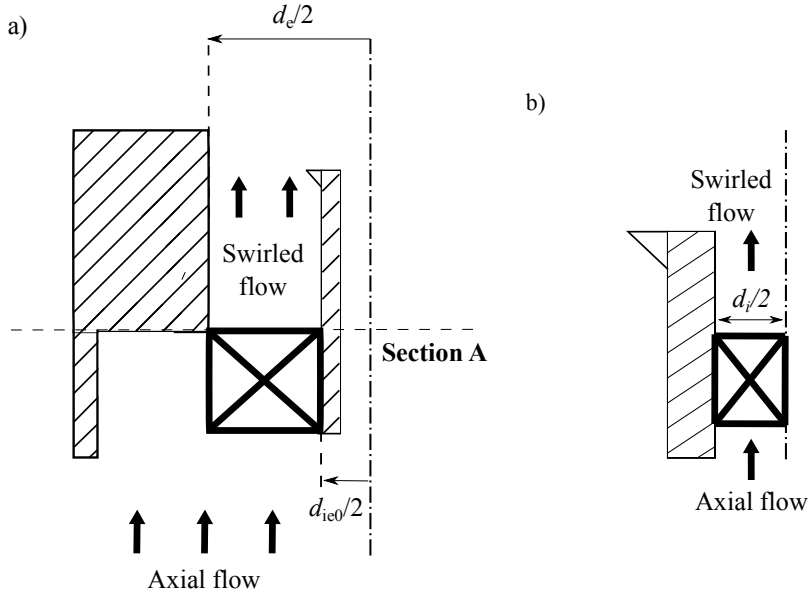


Figure 3: (a) External channel geometry considered for the estimation of the external swirl number S_e . (b) Internal channel geometry considered for the estimation of the inner swirl number S_i .

The swirl number conferred by the radial swirl vane at his outlet (Section A) is given by:

$$S_e = 1/2 \tan(\alpha_{se}) \left(1 - (d_{ie0}/d_e)^4 \right) / \left(1 - (d_{ie0}/d_e)^2 \right) \quad (1)$$

The expression of the swirl number S_i at the outlet of the axial swirler is:

$$S_i = \frac{1}{2} \tan(\alpha_{si}) \quad (2)$$

The estimated values for the swirl numbers are reported in Table 3.

Table 3: Swirl number S_i and S_e at the outlet of the hydrogen and air swirlers respectively.

S_i	S_e
0.6	1.2

3.3 Operating conditions

The two operating conditions for the flames of the phase 2.1 of the TNF HYLON database are reported in Table 4. They are both in atmospheric conditions, the future operating conditions for flames at elevated pressure will be released in an updated version of this document later. Quantities appearing in Table 4 correspond to \dot{m}_j the mass flow rate in g/s, U_b^j the bulk velocity in m/s and T_i^j the temperature in K for air ($j = a$) and hydrogen ($j = h$) injection channels. The thermal power in kW is P_{th} and p corresponds the operating pressure in Pa. The global equivalence ratio is the same for Flames A.1 and L.1: $\Phi_g = 0.421$. The operating point A.1, with a thermal power of $P_{th} = 2.513$ kW, leads to a flame anchored to the H₂ injector lips (Figure 1.a). The flame L.1, with a thermal power of $P_{th} = 5.026$ kW, is V-shaped and aerodynamically stabilized above the injector (Figure 1.b).

Table 4: Operating conditions for flames A.1 and L.1.

Case	\dot{m}_a [g/s]	\dot{m}_h [g/s]	U_b^a [m/s]	U_b^h [m/s]	T_i^a [K]	T_i^h [K]	P_{th} [kW]	Φ_g	p [Pa]
A.1	1.7054	0.02094	11.8	9.3	298	298	2.513	0.421	101325
L.1	3.4108	0.0419	23.7	18.6	298	298	5.026	0.421	101325

3.4 Material of the burner parts

Certain groups may want to perform a coupled simulation of the flow and the temperature in the combustor walls. To do this, the materials of each part of the burner are listed below for thermal simulation of the solid body of the burner (see notations in blue in Figures 4 and 8):

- **Burner body (1):** Stainless steel 304L.
- **Hydrogen injector and both swirlers (2):** Stainless steel 304L.
- **Combustion chamber backplane (3):** Stainless steel 304L.
- **Combustion chamber pillars (4):** Stainless steel 304L.
- **Combustion chamber windows 1 (5):** Stainless steel 304L.
- **Combustion chamber windows 2 (6):** Quartz JSG1 grade.
- **Combustion chamber convergent (7):** Stainless steel 304L.

3.5 Plane of comparison

All measurements will be given in the axial plane $y = 0$ mm of the setup shown in Figure 4 by the red solid line. This plane of comparison must be carefully verified before validation of numerical results using experimental data.

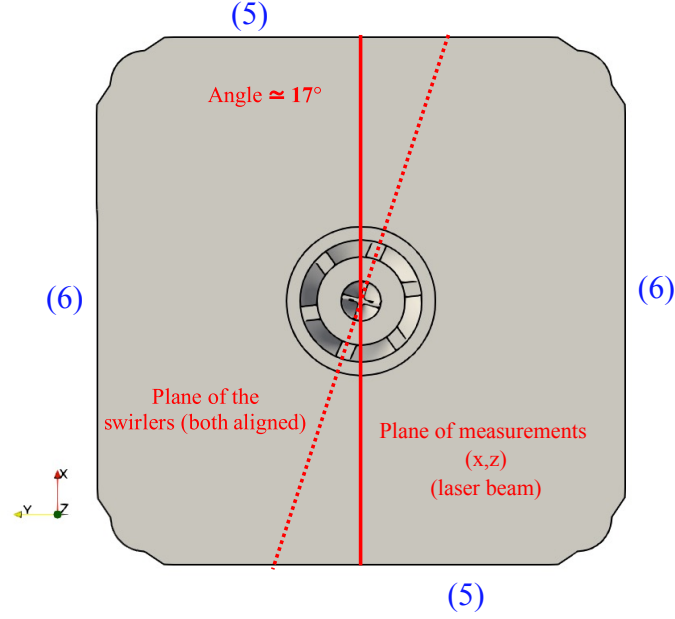


Figure 4: Definition of the comparison plane (x, z) (red solid line).

3.6 Experimental database

Phase 2 of the TNF HYLON database will contain a full set of quantitative experimental measurements conducted under reactive conditions. It includes profiles at different heights of flow velocity, molar fractions of all the main species (N_2 , O_2 , H_2 , and H_2O), flow temperature, and molar fractions of OH and NO, as schematically illustrated in Figure 5. Additionally, the database will include temperatures of the solid components of the combustion chamber at various locations.

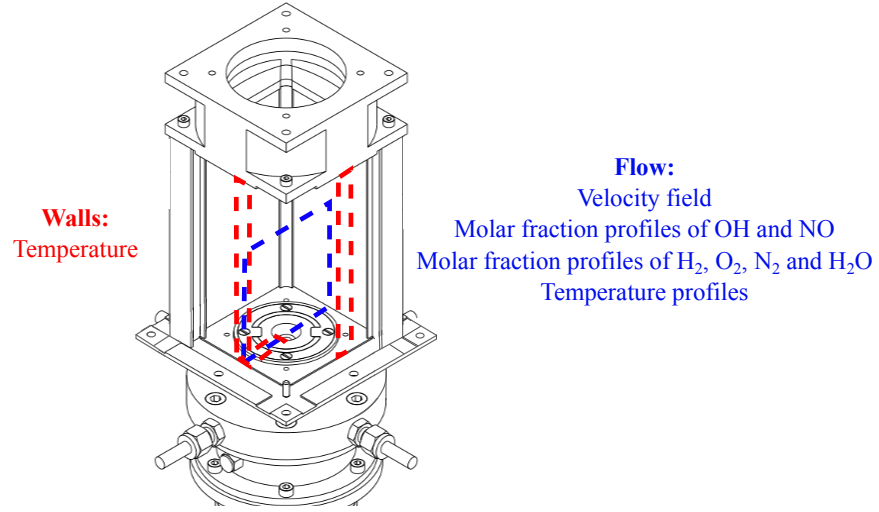


Figure 5: Illustration of the content of the future database.

4 Numerical domain

4.1 CAD

The burner is specially designed to allow precise adjustment of the final experimental assembly. An illustration of the full burner CAD is given in Figure 6.

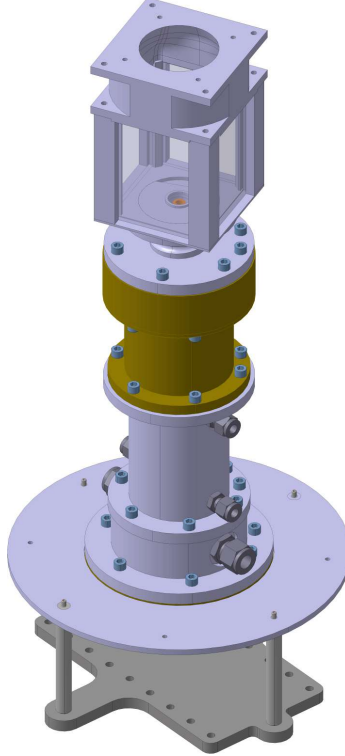


Figure 6: Illustration of the full CAD of the burner setup.

Small modifications and cleaning have been made on the CAD geometry for computational constraints: screws and holes for experiment devices (microphones, thermocouples) have been removed. Some corners have been rounded to avoid meshing issues.

4.2 Geometry validation

To ensure that the CAD data used for CFD matches exactly the experimental one, the geometry of the 3D printed injector has been verified by X-Ray tomography. The CAD files generated before the experiment as built and X-Ray'd have been slightly adjusted to match exactly the injector geometry so that no uncertainty is expected on the geometry. The X-Ray tomography validations have been carried out on the full 3D volume of the air and hydrogen injection block. An illustration of comparison of the X-Ray imaging with the CAD in the plane of symmetry is provided in Figure 7.

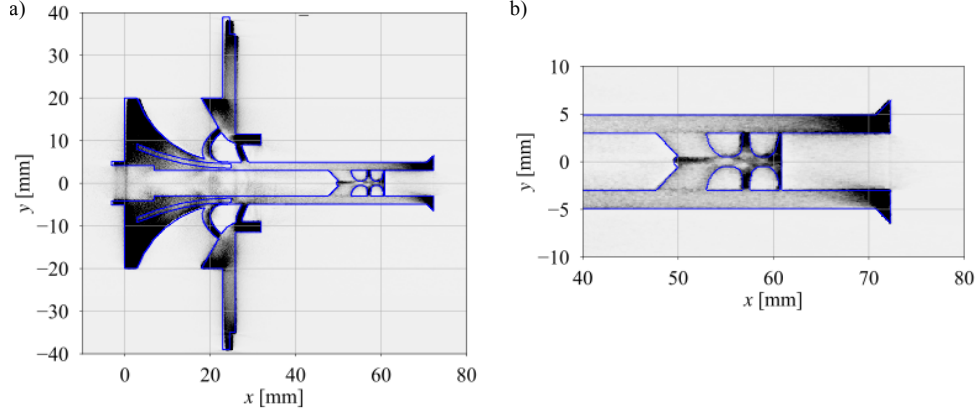


Figure 7: Injector CAD (blue contour) validation by comparison with X-Ray imaging of the experimental part in the plane of symmetry. (a) Full injector cut view. (b) Hydrogen injector cut view.

4.3 Fluid and solid domains

Figure 8 shows the (a) fluid and (b) solid domains available in the database. The fluid domain includes both air and hydrogen swirlers. The solid domain has been provided to allow Conjugate Heat Transfer for teams interested. The solid domain includes the hydrogen swirler, the injector tubes and injector lips, the windows, the corners of the chamber and the convergent at the outlet.

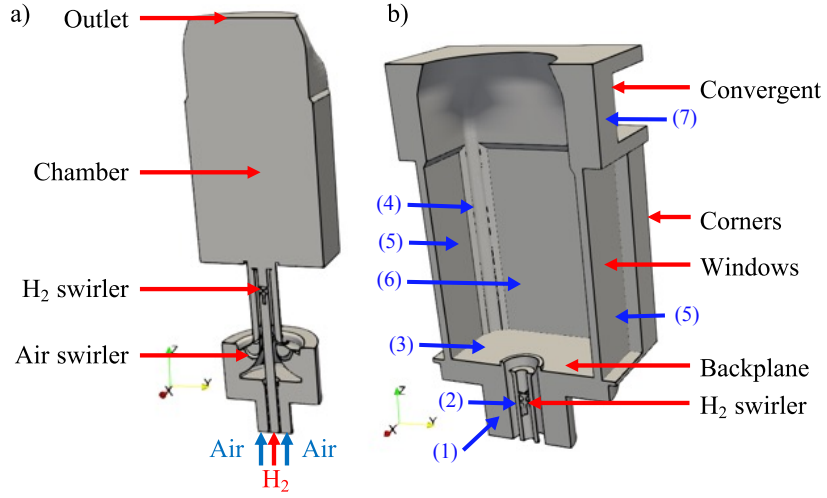


Figure 8: (a) Fluid and (b) solid domains of the numerical setup.

5 Experimental data

5.1 Wall temperatures

Temperature data on the inner wall of the combustion chamber are provided alongside the CAD files. These can serve as thermal boundary conditions for groups not performing coupled simulations with wall heat transfers. Windows and backplane temperatures were measured using a Laser-Induced Phosphorescence (LIP) system (Fig. 9.a), following the method of Guiberti [2]. Measurement surfaces were painted with phosphorescent $\text{Mg}_{3.5}\text{FGeO}_5\text{:Mn}$ powder. A Nd:YAG laser (Litron Nano S 30-60) emitting 30 mJ pulses at 1064 nm and 50 Hz was used. After two frequency doublings, a 266 nm beam with 6 mJ maximum energy was produced; 4 mJ per pulse was used in tests. The beam was directed via two Thorlabs NB1-K04 mirrors and focused using a 1-inch plano-convex $f = 750$ mm lens (Thorlabs LA4716-532). Emitted phosphorescence was collected and focused onto a PMT using two 2-inch plano-convex $f = 500$ mm lenses (Thorlabs LA1380-A), and the wavelength of interest is filtered with a 450 nm longpass filter (Thorlabs FEL0450) and 660 ± 10 nm bandpass filter (Thorlabs FB660-10). Detection used a Hamamatsu PMT H11526-20-NN (gain: 0.38 V) and a Tektronix DPO4104B oscilloscope (2.5 MHz sampling, 2 s per point). Temperatures were derived from phosphorescence decay times, calibrated from 300–1000 K using a painted type K thermocouple and an air heater. Results represent averages over 100 laser shots, with uncertainty estimated from post-processing variability.

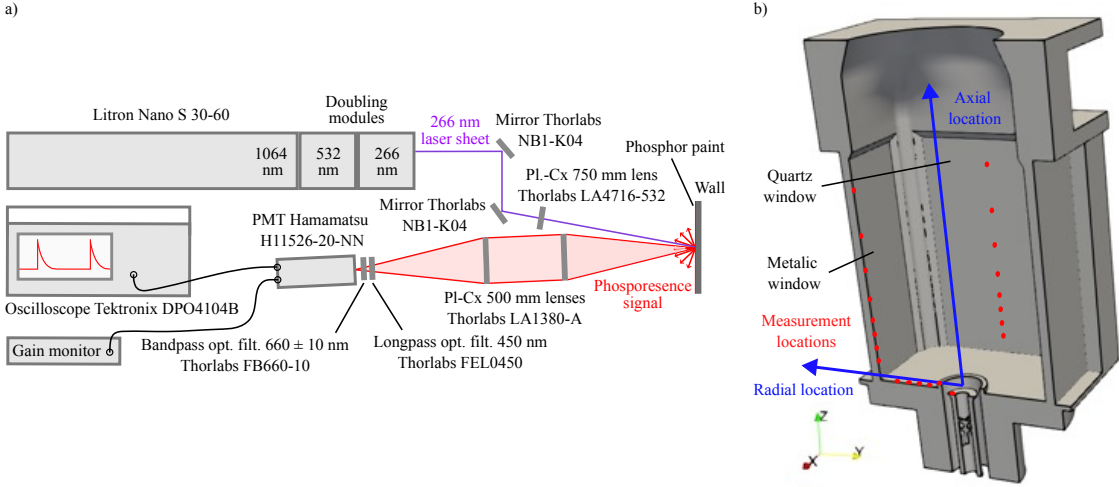


Figure 9: (a) Schematic of the LIP experimental setup. (b) Illustration of measurement locations of the wall temperature of the combustion chamber.

A schematic illustration of the measurement locations is shown in Fig. 9.b. Wall temperature measurements are taken at the inner side of the walls of the combustion chamber. Data are taken at the hydrogen and air injector lips, at 4 locations on the combustion chamber backplane (on the axis $x = 0$ mm) and 8 locations on the metallic (on the axis $x = 0$ mm) and quartz windows (on the axis $y = 0$ mm).

6 Content of the folder

The name of the folder corresponds to the version of the data file, referenced as HYLON_TNF_YEAR.MONTH.Phase2-1, for data made available at year YEAR and month MONTH. Example: HYLON_TNF_2025_04.Phase2-1 for data made available in April 2025. As for the HYLON Phase 1, the folder "HYLON_TNF_2025_05.Phase2-1" is organized as follow:

- Geometry_Fluid_HYLON_TNF_2025_02.Phase2.igs → *CAD file of the fluid domain*
- Geometry_Solid_HYLON_TNF_2025_02.Phase2.igs → *CAD file of the solid domain*
- [HYLON_TNF_2025_05.Phase2-1.PDF.pdf](#) → *Describing PDF file*
- Flame A1 → Directory with the data of flame A1.
 - A1_Wall_Temp → Directory with the temperatures of the gas and the walls at the locations described Section 4.3.
 - * T_wall.backplane → Wall temperature on the injector and the backplane of the combustion chamber.
 - * T_wall.chamber.metal → Wall temperature on the metallic window of the combustion chamber.
 - * T_wall.chamber.quartz → Wall temperature on the quartz window of the combustion chamber.
- Flame L1 → Directory with the data of flame L1.
 - L1_Wall_Temp → Directory with the temperatures of the gas and the walls at the locations described Section 4.3.
 - * T_wall.backplane → Wall temperature on the injector and the backplane of the combustion chamber.
 - * T_wall.chamber.metal → Wall temperature on the metallic window of the combustion chamber.
 - * T_wall.chamber.quartz → Wall temperature on the quartz window of the combustion chamber.

,

7 Published work on HYLON burner

The HYLON injector technology was patented in collaboration with Safran Helicopter Engine (SHE) [11, 10].

The impact of the internal swirl level S_i and the recess distance z_i on flame stabilization has been investigated in Marragou *et al.* [9] for CH₄/H₂/air flames and in Marragou *et al.* [5] for H₂/air flames.

The transition between lifted to anchored flame has been studied with a model described in Marragou *et al.* [5]. Improvement of this model and comparisons between predictions and measurements were carried out in Marragou *et al.* [7]

Flame stabilization and NO_x emissions are further investigated in Magnes *et al.* [3] for high-temperature of air injection. The interplay between unburnt H₂ and NO_x emissions are studied in Magnes *et al.* [4].

Some of the data presented in the previous phase of the TNF HYLON database were compared to numerical flow simulations in Aniello *et al.* [1]. Simulations have been recently carried out for analysis of NO_x formation mechanisms by Vilesby *et al.* [12].

Mixing in cold flow conditions is experimentally investigated in Marragou *et al.* [8]. First investigations of the flame stabilization and pollutant emissions have been recently carried out by Marragou *et al.* [6] at elevated pressure in a configuration similar to the one for the phase 2 of the TNF HYLON database.

8 Acknowledgements

The team gratefully acknowledges Domingo Lattanzi Sanchez for the realization of the X-ray tomography of the injector at KAUST.

References

- [1] A. Aniello et al. “Experimental and numerical investigation of two flame stabilization regimes observed in a dual swirl H₂-air coaxial injector”. In: *Combustion and flame* 249 (2023), p. 112595.
- [2] T. Guiberti. “Analysis of the topology of premixed swirl-stabilized confined flames”. PhD thesis. Ecole Centrale Paris, 2015. URL: <https://theses.hal.science/tel-01154870>.
- [3] H. Magnes et al. “Impact of preheating on flame stabilization and NO_x emissions from a dual swirl hydrogen injector”. In: *Journal of Engineering for Gas Turbines and Power* 146.5 (2023), p. 051004.
- [4] H. Magnes et al. “Interplay between unburned emissions and NO_x emissions from a dual swirl hydrogen air injector”. In: *Journal of Engineering for Gas Turbines and Power* 147.6 (2025), p. 061013.
- [5] S. Marragou et al. “Experimental analysis and theoretical lift-off criterion for H₂/air flames stabilized on a dual swirl injector”. In: *Proceedings of the Combustion Institute* 39.4 (2023), pp. 4345–4354.
- [6] S. Marragou et al. “Flame stabilization and pollutant emissions from a H₂/air dual swirl coaxial injector at elevated pressure”. In: *International Journal of Hydrogen Energy* 100 (2025), pp. 163–172.
- [7] S. Marragou et al. “Modeling of H₂/air flame stabilization regime above coaxial dual swirl injectors”. In: *Combustion and Flame* 255 (2023), p. 112908.
- [8] S. Marragou et al. “Near-field mixing in a coaxial dual swirled injector”. In: *Flow, Turbulence and Combustion* 114 (2024), pp. 221–242.
- [9] S. Marragou et al. “Stabilization regimes and pollutant emissions from a dual fuel CH₄/H₂ and dual swirl low NO_x burner”. In: *International Journal of Hydrogen Energy* 47.44 (2022), pp. 19275–19288.
- [10] S. Richard et al. *Device for injecting dihydrogen and air (WO Patent No WO2023057722A1)*. Institut National de la Propriété Industrielle, 2023.
- [11] S. Richard et al. *Dispositif d’injection de dihydrogène et d’air (FR Patent No FR3127988A1)*. Institut National de la Propriété Industrielle, 2021.
- [12] M. Vilespy et al. “Analysis of the origin of NO_x emissions in non premixed dual swirl hydrogen flames”. In: *Combustion and Flame* 273 (2025), p. 113925.